Estimation of Tropospheric Fluctuations Using GPS Data

C. J. Naudet
Tracking Systems and Applications Section

This article reports on a method of extracting tropospheric turbulence statistics from the Global Positioning System (GPS) Flinn database. The elevation and site dependence of the GPS residuals are shown to agree with the expectations of troposphere delay fluctuations. The GPS residuals are shown to have temporal statistics that are consistent with the assumed turbulence model. The turbulence parameter, C_n, is extracted from the GPS residuals and is found to be consistent with both water vapor radiometer and very long baseline interferometry measurements. Seasonal and diurnal variations in C_n were observed to be consistent with other measurements and compared well with a simple wet refractivity model. This technique for obtaining C_n from GPS data may be useful for several classes of Ka-band (32-GHz) radio science experiments, as they will be limited by tropospheric phase fluctuations.

I. Introduction

Tropospheric delay fluctuations are a dominant error source for most classes of Ka-band (32-GHz) radio science experiments and high-frequency radio interferometry. This article reports on the use of the Global Positioning System (GPS) Flinn database to estimate the level of the tropospheric fluctuations at sites with GPS receivers. Development of a large database of the tropospheric seasonal, diurnal, and site fluctuations will serve many purposes. These measurements could help in the understanding of Ka-band telemetry array error budgets and allow for improved observable covariances for radio science, very long baseline interferometry (VLBI), and Doppler measurements. Improved estimates of observable covariances lead to more accurate parameter estimates and reduced parameter variance. In addition, knowledge of seasonal, diurnal, and site dependence of the tropospheric fluctuations could assist in the optimal scheduling of planned radio science experiments. The GPS global network database is ideally suited for use in the development of troposphere fluctuation statistics.

The GPS global network consists of over 20 satellites in 6 equally spaced orbital planes at an altitude of ∼20,000 km and a worldwide distribution of ground receivers, presently over 50. Typically, from four to eight satellites are in view at any time. GPS satellites transmit at frequencies L1 and L2 (1.227 and 1.575 GHz). The dual-frequency (ionosphere-free) GPS carrier phase data received on the ground may be written as

$$\Phi = \frac{d_{gps}\nu_{carrier}}{c} + \Delta t_{clock}\nu_{carrier} + \frac{\tau_{trop}\nu_{carrier}}{c} + noise + bias \tag{1}$$

where d is the range to the satellite, ν is the carrier frequency, c is the speed of light, Δt is a clock offset term, and τ_{trop} is the tropospheric delay along the line of sight to the satellite. The data obtained from the ground receivers are used in a global estimation for satellite orbits, receiver locations, transmitter clock offsets, zenith tropospheric delays, and other parameters. In addition, for each satellite–receiver combination, a residual is saved for every observation (the sampling time was ∼7.5 min for data analyzed in this article). The residuals are the delay difference between each observation and its computed predicted value from the model. The rms of the residuals, averaged over a day, is ∼0.3 cm. At JPL, the GPS Flinn analysis team produces the daily solution sets and residuals. Data exist from June 1992 to the present and are obtained 24 hours a day in all weather conditions.[1]

Presently, an estimation of GPS zenith troposphere delay and other parameters is carried out by a global estimation process (a sequential pseudo-epoch state process noise filter). Parameter estimates and residuals are calculated every 7.5 min, the sampling time (i.e., one mean zenith tropospheric delay is estimated every sampling interval for each ground site). It is expected that the residuals will have significant contributions from the tropospheric fluctuations that occur over time scales shorter than the sampling time (frequencies >2 mHz). The contribution to the residuals from lower-frequency tropospheric fluctuation components is more complex and depends upon the details of the GPS global filter/estimation algorithm. The GPS global estimation algorithm currently models the stochastic troposphere by a first-order temporal Gauss–Markov random process, although there is strong evidence [1] that the troposphere should be modeled by the spatial and temporal Kolmogorov turbulence theory. Since the Kolmogorov spatial and temporal correlations are not included in the GPS global estimator, it is expected that a portion of the low-frequency tropospheric fluctuations will remain in the GPS residuals. The hypothesis is formed that the GPS residuals are dominantly tropospheric delay fluctuations.

The organization of this article is as follows: In the next section, I discuss the origin of the GPS residuals used here and demonstrate that the variance of the residuals is proportional to $sin^2(\theta)$, as expected if there were significant tropospheric components to the residual. In Section III, the Allan deviation and probability density function for the GPS residuals are computed and shown to be consistent with that expected from a Kolmogorov turbulent process. Section IV discusses the extraction of tropospheric fluctuation statistics from the GPS database. A thorough discussion of the seasonal, site, and diurnal dependence of the turbulence parameter, C_n, is given in Section V, and a comparison with a mean wet refractivity model is discussed in Section VI. Finally, the summary is given in Section VII.

II. GPS Residuals

The satellite viewing angles for a typical day (February 4, 1994) at the Goldstone GPS site are shown in Fig. 1(a). The GPS satellites in view at any moment are scattered over wide angles in azimuth and elevation. Histograms of the elevation (bin size = 1 deg) and azimuth (bin size = 4 deg) are shown in Figs. 1(b) and 1(c), respectively. The GPS satellites are distributed approximately uniformly in azimuth and are peaked at ∼25 deg in elevation. To avoid multipath effects, the Flinn analysis team has chosen an elevation cutoff of ∼20 deg.[2] Since the tropospheric delay fluctuations at time scales greater than ∼200 s are expected to be linearly proportional to the air mass between the satellite and the GPS receiver,[3] it is expected that the magnitude of fluctuations in the residual will have a $\sim 1/\sin\theta$ dependence, where θ is the elevation angle. Figure 2 shows the GPS residual rms dependence on elevation angle for a 10-day period, June 12–21, 1994, for four different sites: Alberthead, British Columbia (B.C.); Goldstone, California;

[1] The full details of the GPS Flinn analysis can be found in F. H. Webb and J. F. Zumburge, *An Introduction to GIPSY/OASIS II*, JPL D-11088 (internal document), Jet Propulsion Laboratory, Pasadena, California, July 1993.

[2] The GPS Flinn team changed the elevation cut to 15 deg and the interval sampling time to 300 s for all data processed after November 1, 1995. In addition, improvements in various software models were implemented at that time.

[3] R. Linfield, "Troposphere Delay Variance as a Function of Elevation Angle and Time Span," Deep Space Tracking Systems Group Note (internal document), Jet Propulsion Laboratory, Pasadena, California, December 2, 1994.

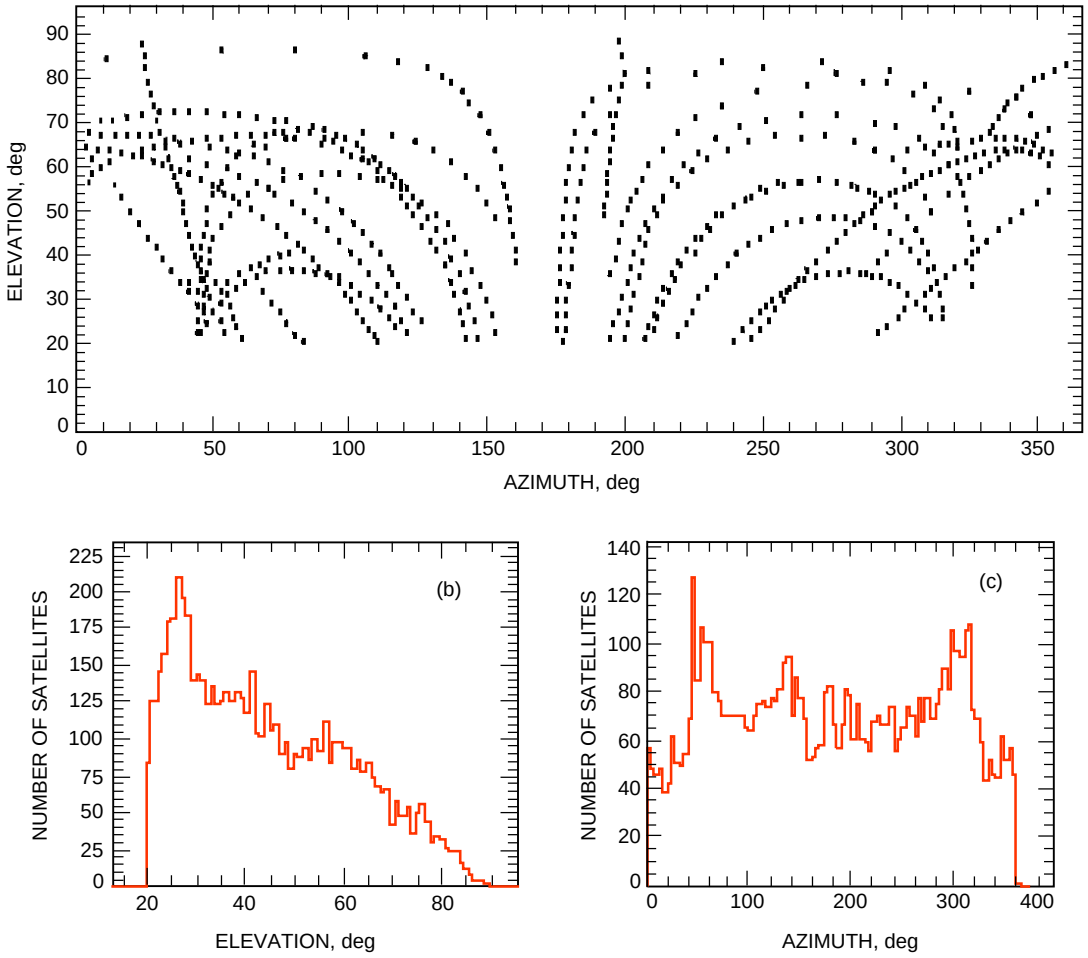

Fig. 1. February 4, 1994, Goldstone (a) satellite viewing angles, (b) GPS satellite elevation distribution, and (c) GPS satellite azimuth distribution.

Fortaleza, Brazil; and Kourou, French Guiana (F.G.). The sites at Fortaleza and Kourou are in tropical regions that on average are much wetter than the other two sites, Alberthead and Goldstone. Fortaleza and Kourou have a 10-day averaged rms residual delay ($\langle rms \rangle$) of 0.85 and 0.92 cm, respectively. The Goldstone and Alberthead sites are found to have $\langle rms \rangle$ values of 0.34 and 0.51 cm, approximately a factor of two to three smaller than the wet sites. The solid line on each figure is a least-squares fit using the function form

$$rms^2 = a + \frac{b}{\sin^2(\theta)} \tag{2}$$

Good agreement is found with the assumption of a constant and an airmass-dependent contribution $(1/\sin\theta)$ to the variance of the residuals. This *may* correspond to a nontropospheric (constant) and a tropospheric component ($\propto 1/\sin\theta$). The least-squares fit to the Alberthead site yields $a = 0.16$ cm^2 and $b = 0.07$ cm^2, which yields a $1/\sin\theta$ component approximately twice as large as the constant component at the peak elevation angle of 25 deg. Both a and b were found to vary with both site and season; typically, factors of 2 to 3 are found from least-square estimates. If the constant and $1/\sin\theta$ terms do correspond to nontropospheric and tropospheric error sources, then it may be possible to isolate

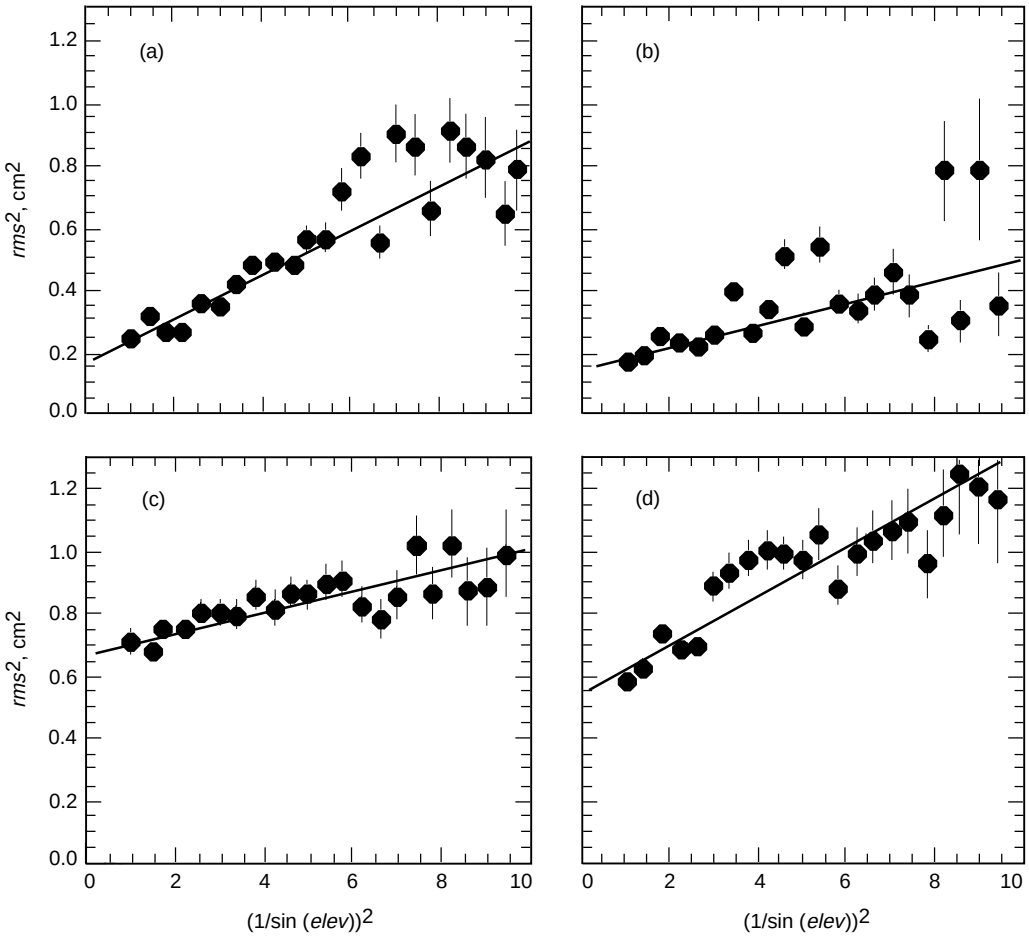

Fig. 2. Elevation dependence of the GPS residuals: (a) Alberthead, B.C., (b) Goldstone, California, (c) Fortaleza, Brazil, and (d) Kourou, F.G.

the tropospheric fluctuation component by filtering the data based on elevation angle (this has been left for future study). Other sources of possible error, such as multipath or TurboRogue receiver system temperature, may also have approximately a $1/\sin\theta$ dependence, but it is not expected that these terms will have the site, seasonal, and diurnal dependence or the temporal statistics expected for tropospheric effects. Rather than rule out all possible GPS error sources, which would entail a detailed study of the GPS error budget, this article attempts to show that the residuals' fluctuations are *consistent* with being tropospheric turbulence.

III. Residual Statistics

A random function, f, observed as a time series may be characterized by a measure of its Allan variance, the average fractional deviation stability:

$$[\sigma_y(\Delta t)]^2 = \frac{\langle [f(t+2\Delta t) - 2f(t+\Delta t) + f(t)]^2 \rangle}{2\Delta t^2} \tag{3}$$

where Δt are the time intervals between the measurements of f.

The power law dependence of the Allan standard deviation (ASD) upon time interval is well known for various stochastic noise processes; white noise and random walk have a -1 and $-1/2$ power law dependence, respectively. Kolmogorov turbulence theory predicts a power law dependence of $-2/3$ for tropospheric delay fluctuations with time scales greater than the troposphere height, h, divided by the average wind speed, v: $\Delta t > h/v$ ($\sim$200 s) (see [1]). The GPS Flinn database does not estimate the tropospheric delay for each satellite but does estimate a single zenith tropospheric delay for each time interval at each site. The ASD for the estimated zenith tropospheric delay as a function of the sampling interval is shown in Fig. 3 for January 8, 1994. A significant disagreement with Kolmogorov turbulence theory is observed: At short intervals, $t < 20,000$ s, the dependence has random-walk characteristics consistent with what is assumed in the global estimation process filter; at longer times, the dependence switches rapidly to white noise. We can attempt to obtain the correct statistics by reconstructing the tropospheric delay for each satellite as

$$\tau_c(t) = \tau(t)_{res} + \frac{\tau_z(t) - \langle \tau_z \rangle}{\sin(\theta(t))} \tag{4}$$

where $\tau(t)_{res}$ is the GPS residual for that satellite, $\tau_z(t)$ is the zenith troposphere estimate at that site, and $\langle \tau_z \rangle$ its time average.[4] The elevation dependence is corrected by the inclusion of the $1/\sin\theta$ term. The ASD for the corrected satellite tropospheric delay as a function of time interval is shown in Fig. 4 for the GPS data from April 4, 1994, at four different sites. A power law fit to each site (for $\Delta t < 8000$ s) yields an estimated slope of 0.75 ± 0.05 s^{-1}, consistent with the Kolmogorov turbulence value of 2/3. Figure 4 indicates an observable difference in the magnitude of the ASD curve between different sites. The wetter sites (Kourou and Fortaleza) typically have an ASD magnitude that is approximately a factor of 2 to 3 larger than the drier sites (Goldstone and Alberthead).

An additional method of statistical comparison of turbulence phenomena is to examine the probability density function (pdf) of the fluctuations [2]. The tropospheric delay fluctuations are defined as the difference in the tropospheric delay between successive sampling times, 450 s. For GPS data, this is calculated using $\tau(t)_{res}$.[5] If a time series is distributed as random walk (or any first-order Gauss–Markov process), then its fluctuation pdf is the normal distribution. However, the expected probability distribution function for a true turbulent time series is a non-Gaussian distribution. These non-Gaussian pdf's are well modeled by stretched exponential distributions [2] or Levy–Pareto distributions [3]. Hence, the frequency distributions of satellite residuals should indicate the underlying statistics. However, the elevation dependence must first be removed. This can most easily be done by mapping the residuals to zenith:

$$R_z(i,t) = \tau_i(t)_{res} m\left[\theta(t), i\right] \tag{5}$$

where R_z is the zenith mapped residual for satellite i at time t and $m[\theta(t), i]$ is an elevation mapping function [4], ($\sim\sin\theta$) for satellite i at elevation θ. Figure 5 plots the satellite zenith residual pdf; the black dashed curve is a least-squares Gaussian fit. Clearly, the GPS zenith residual pdf has tails that are very non-Gaussian. The solid curve in Fig. 5 is a calculation for a Kolmogorov turbulence model pdf [3,5]. A least-squares fit of the GPS zenith residual pdf using a Pareto distribution yields a characteristic exponent, α, of $\sim$3.0, in agreement with the expected value from Kolmogorov turbulence (see details in

[4] Since we are concerned only with fluctuations, the reconstructed tropospheric delay is defined about a mean value of zero. The time average is over 24 h. It should be noted that the $\langle \tau_z \rangle$ term acts as a high-pass filter; all $\tau_z(t)$ fluctuations that occur over time scales shorter than the averaging period will contribute to the fluctuations in $\tau_c(t)$. By adjusting the running average time window, an optimal $\tau_c(t)$ can be constructed.

[5] It is equivalent to use either $\tau_{res}(t)$ or $\tau_c(t)$ since the first differences of $\tau_z(t)$ are very Gauss-like.

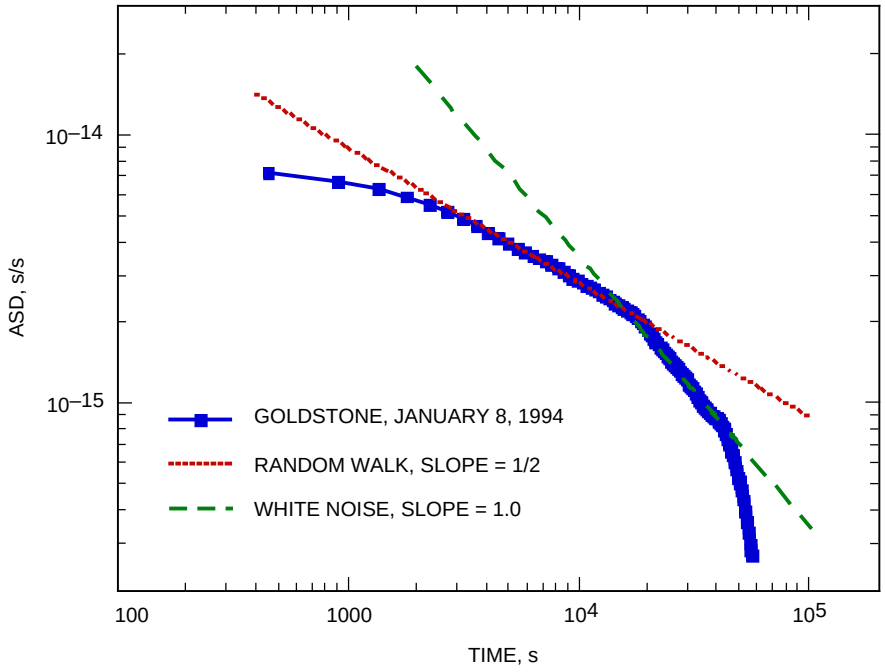

Fig. 3. The Allan standard deviation of the GPS tropospheric delay estimate.

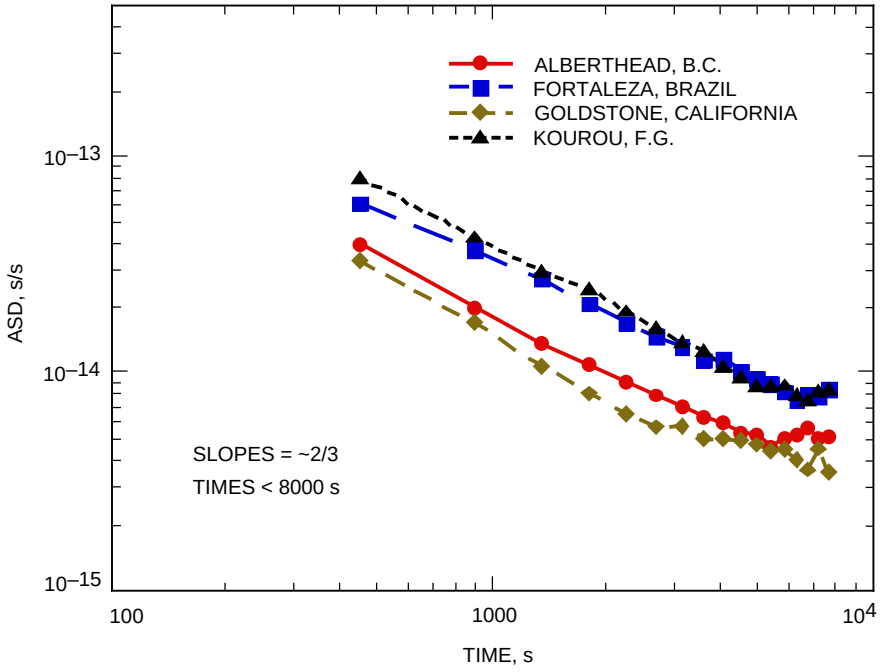

Fig. 4. The spectrum (ASD) of the GPS residuals.

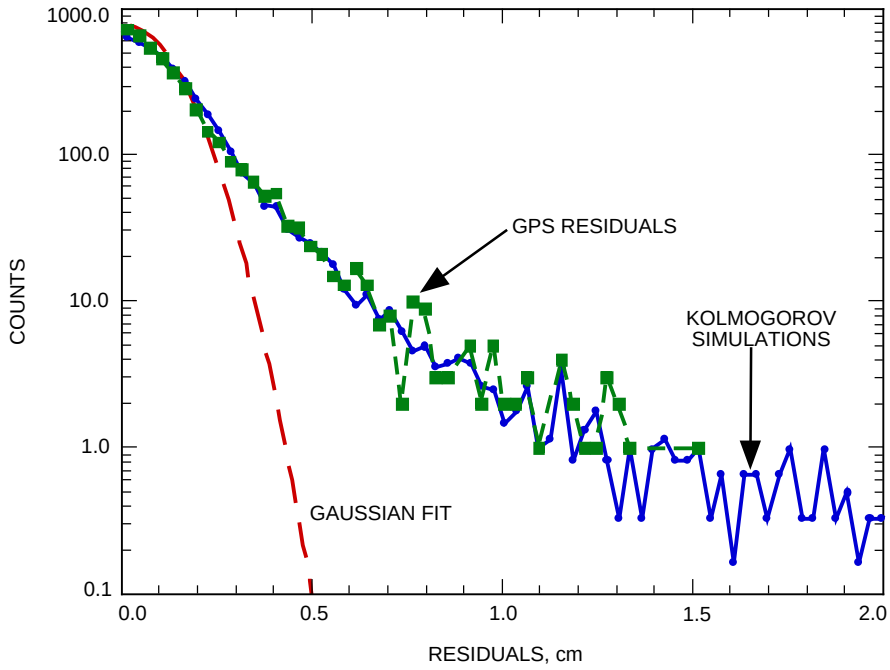

Fig. 5. The probability density function of the GPS residuals.

Appendix A). The GPS zenith residual pdf is clearly in much better agreement with the Kolmogorov pdf, consistent with the interpretation of an underlying Kolmogorov turbulence.[6] In addition, a stronger statement can be made by noting that if the sampling time is increased (e.g., by a factor of from 10 to 4500 s), the pdf is still observed to have non-Gaussian tails and the pdf follows the scaling law of Eq. (A-4). This type of power law pdf scaling is expected for scale invariant intermittency cascade models of turbulence.

IV. Estimation of Tropospheric Fluctuations

The line-of-sight delay fluctuations of an initially plane wave front that traverses the atmosphere can be characterized by the structure function of delay:

$$D_\tau(\mathbf{R}) = \langle [\tau(\mathbf{r}+\mathbf{R}) - \tau(\mathbf{R})]^2 \rangle \tag{6}$$

where $\mathbf{r}$ is the line-of-sight vector, $\mathbf{R}$ is a displacement vector, and the angle brackets represent an ensemble average. In addition, we assume that $D_\tau(\mathbf{R})$ depends only on $|\mathbf{R}| = R$ and that the turbulence is locally homogeneous and isotropic. The tropospheric delay may be defined as

$$\tau = \frac{1}{\sin\theta} \int \chi[\mathbf{x} + \mathbf{r}(z)] dz \tag{7}$$

where χ is the refractivity and $\mathbf{r}(z)$ is the vector from the ground in the direction of interest, at height z. Then the variance of delay over a time interval T is

[6] The reader should be reminded of a subtle point: the power law dependence of the tropospheric delay structure functions is 2/3 ($\alpha = 3$) only for times larger than 200 s ($V_{wind} =\sim 10$ m/s); for shorter times, the power law goes as 5/3 ($\alpha = 6/5$) (see [1]).

$$\sigma^2(T) = \frac{1}{T^2}\int (T-t)D_\tau(t)dt \tag{8}$$

(See Eq. (B-3) of [1].) An essential component in our assumptions is that tropospheric delay fluctuations are well represented by the frozen flow turbulence model. The two primary assumptions in this model are as follows. First, the spatial structure of index of refraction fluctuations follows Kolmogorov turbulence theory [6,7]:

$$D_\chi(R) = \langle[\chi(r+R) - \chi(R)]^2\rangle = \left(C_n R^{1/3}\right)^2 \tag{9}$$

where C_n (the structure constant) characterizes the rockiness of the spatial inhomogeneity of the troposphere. Second, as regards frozen flow, temporal fluctuations are due to spatial patterns moving over the site by the wind.

The first assumption implies that the delay standard deviation, σ_τ, and the Allan standard deviations, $\sigma_y(\Delta t)$, vary linearly with the structure constant:

$$\left.\begin{aligned} \sigma_\tau &\propto \mathbf{C_n} \\ \sigma_{\mathbf{y}}(\mathbf{\Delta t}) &\propto \mathbf{C_n} \end{aligned}\right\} \tag{10}$$

The second assumption, along with the flat slab approximation (the assumption that the structure function, D_χ, is independent of altitude up to some height, h), allows us to model both σ_τ and $\sigma_y(\Delta t)$ by three parameters: the slab height (typically 2 km), the average slab wind velocity (8 to 10 m/s), and C_n (mean DSN value of 1.1×10^{-7} m$^{-1/3}$).

If the ensemble wind velocity and slab height are used at each site, then under most circumstances, the magnitude of the fluctuations can be characterized by one parameter, C_n, the structure constant [1]. The tropospheric delay has both wet and dry components. The dry component is approximately 2 m at zenith and varies slowly and smoothly. The wet component ($\sim$10 cm) is due to water vapor and has large temporal and spatial random variations. The extracted structure constant, C_n, will be composed of wet and dry components with the wet component dominating (greater than $\sim$80 percent). Ideally, C_n is a *strict constant* over all the temporal and spatial ranges of interest, characterizing the strength of the stochastic (not systematic) tropospheric fluctuations. However, tropospheric fluctuations are driven by temperature differences, wind velocity, and water vapor pressure fluctuations, so we would expect to observe site, seasonal, and diurnal C_n systematic dependencies. The GPS Flinn database may help us develop an understanding of these systematic variations.

An extraction of the structure constant for a given site can be obtained by a calculation of the theoretical zenith tropospheric delay standard deviation, $\sigma_{theory}(T)$, for some nominal value of C_n (full details are given in Appendix B) and a calculation of the actual $\sigma_{residual}$ measured with the GPS for a given time interval, T:

$$C_n(T) \propto \frac{\zeta\ \sigma_{residual}(T)}{\sigma_{theory}(T)} \tag{11}$$

where ζ is a correction factor (currently $\zeta = 1$) that depends upon the fraction of the tropospheric fluctuations contained in the residuals and the proportion of the residuals that consists of nontropospheric error sources (i.e., multipath, instrumental, ionosphere, etc.). The value of ζ may change depending upon

any changes in the GPS Flinn analysis procedure or software. The time interval chosen for the C_n extraction in this article was 450 s, the sampling time. The extracted C_n's are then averaged over longer time periods: 2 hours, 4 hours, daily, or longer.

V. GPS C_n Results

A GPS-extracted C_n time series is shown for the Goldstone site during a 10-day period from June 12 to 21, 1994, in Fig. 6(a); a 4-hour averaging period is used. The average value for this 10-day period was found to be $\sim 0.95 \times 10^{-7}$ m$^{-1/3}$. The absolute magnitude is consistent with what is experimentally obtained from other measurements, for instance, the yearly average Goldstone value obtained through VLBI estimation [1,8]. Diurnal variations of 25 to 50 percent are observed with the largest C_n amplitudes observed at approximately 4:00 p.m. local time. The power spectrum of the time series [9], Fig. 6(b), also shows a strong diurnal power amplitude. Examination of the other sites shows similar day and night behavior. Studies of phase stability at the very large array (VLA) [10], water vapor radiometer (WVR) fluctuations in Puerto Rico,[7] and tropospheric scintillations at 14 and 11 GHz [11] all find diurnal variations consistent with the present observations.

The extracted C_n time series for a much longer period of time, from January 1 to August 1, 1994, are shown in Fig. 7 for both the Alberthead, B.C., and Fortaleza, Brazil, sites, using 2-hour averages. The 9-month C_n averages are 1.9×10^{-7} m$^{-1/3}$ and 1.3×10^{-7} m$^{-1/3}$ for Fortaleza (wet site) and Alberthead (dry site), respectively. The rms of the C_n is found to be directly proportional to the average value. From Fig. 7, we conclude that the extracted C_n has a dynamic range of at least a factor of 5 and an upper estimate of the noise floor is less than 50 percent of the average C_n value. Comparison with winter WVR data at the Goldstone site (see below) suggests that the noise floor could be much lower.

Two-hour extracted C_n averages in Fig. 7 illustrate that the diurnal variations at both sites dominate over the smaller seasonal trends and somewhat mask the site differences. By using a 20-day moving average to filter out the high-frequency components, the seasonal variations can be extracted. An increase of approximately 10 percent from winter to summer is observed at the Alberthead, B.C., site, and a decrease of approximately 10 percent is found at the Fortaleza site. These seasonal variations are smaller than what is expected from both WVR and VLBI experiments, where a factor-of-two variation about the annual mean is typically measured. However, the sign of the seasonal change is consistent with the known meteorological patterns at those sites.

The seasonal dependence of the day and night C_n values is examined in Fig. 8 for Goldstone. The figure shows the 2-hour averaged C_n data divided into a day period (1 p.m. through 9 p.m. local time) and a night period (12 p.m. through 8 a.m. local time),[8] then smoothed with a 20-day moving average process. The night period shows little variation in C_n between the winter and the summer. The day period, however, shows an increase of approximately 25 percent in the C_n value from the winter to summer periods. This seasonal dependence analysis was checked by taking the entire 2-hour C_n time series and dividing it up into monthly periods, and then calculating the power spectral density for each monthly period. The amplitude of the diurnal period is the strongest for the summer months of June and July and weakest in the November-to-January time period.

Finally, a direct comparison with WVR estimates of tropospheric fluctuations can be made for the Goldstone site. Throughout 1994, an R6 WVR acquired data at DSS 13, roughly 20 km from the DSS-15 GPS TurboRogue. The results have recently been published [8]. To compare these with the GPS

[7] D. E. Hogg, "A Study of the Water Vapor Fluctuations at Selected Sites in Puerto Rico," VLB Array Memorandum 312, Arecibo Observatory, Puerto Rico, January 24, 1984.

[8] The day and night time periods were selected to agree with those used in [8].

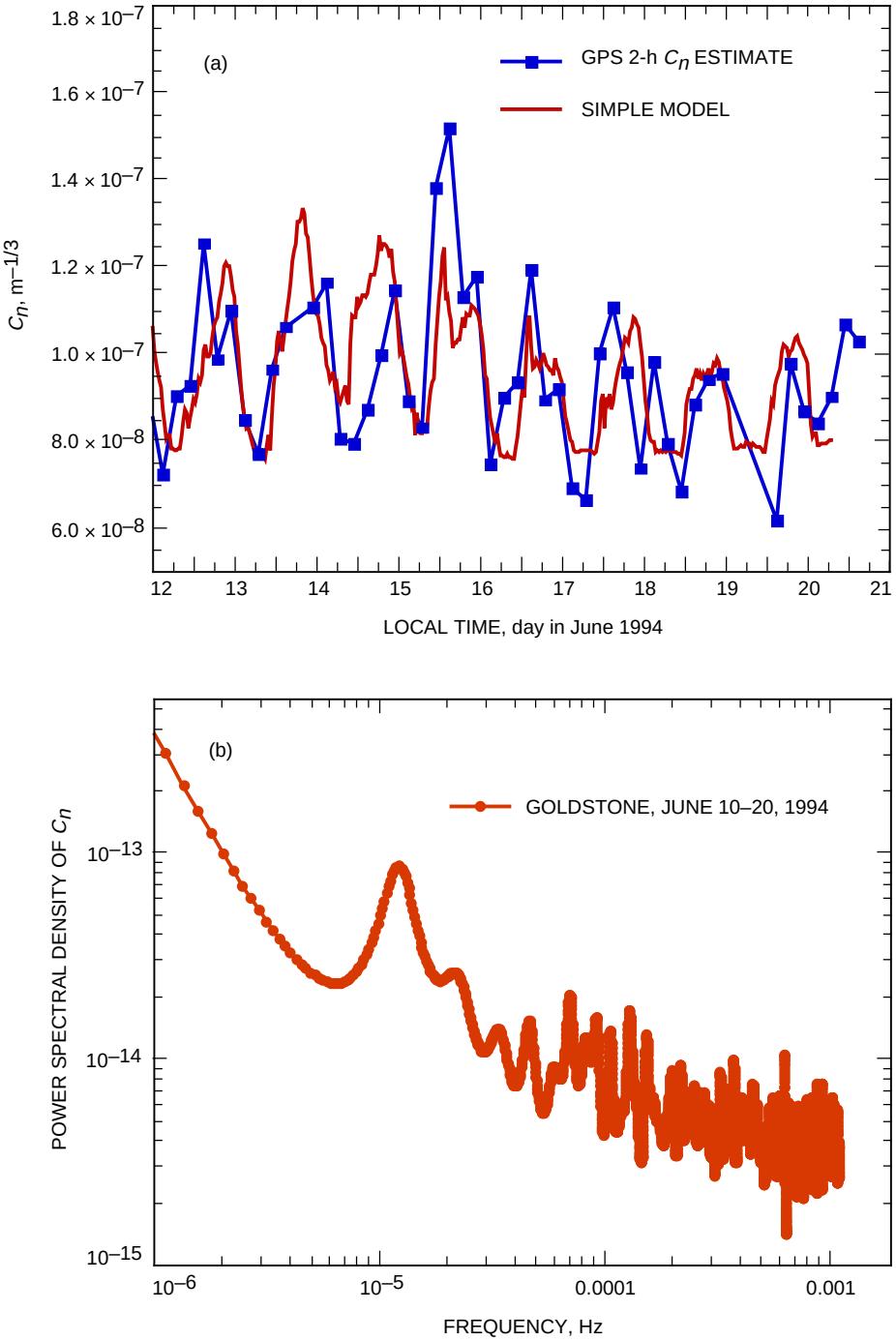

Fig. 6. A C_n time series: (a) a comparison of C_n data and the model and (b) the power spectral density of C_n.

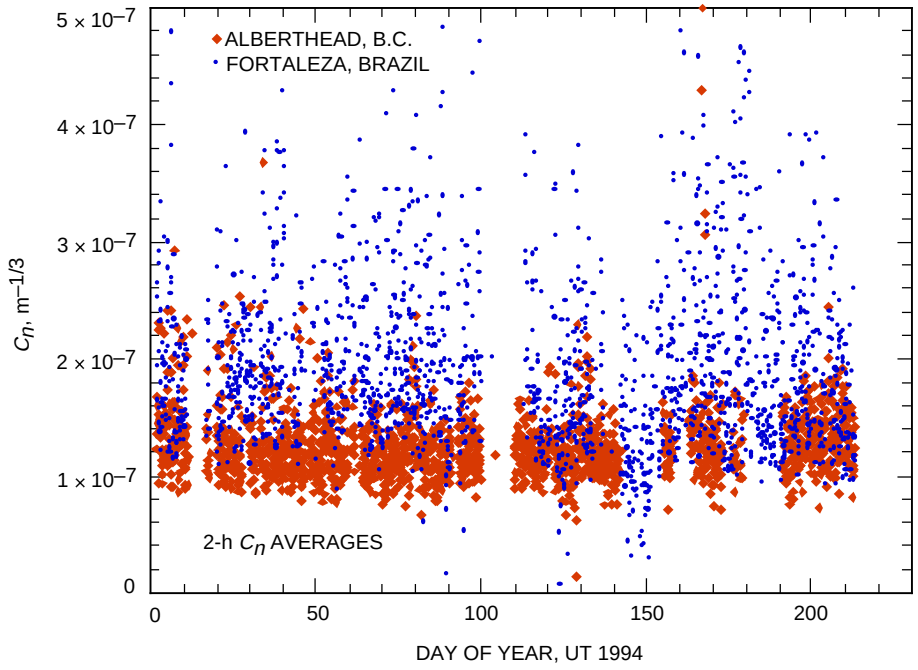

Fig. 7. Seasonal C_n variations.

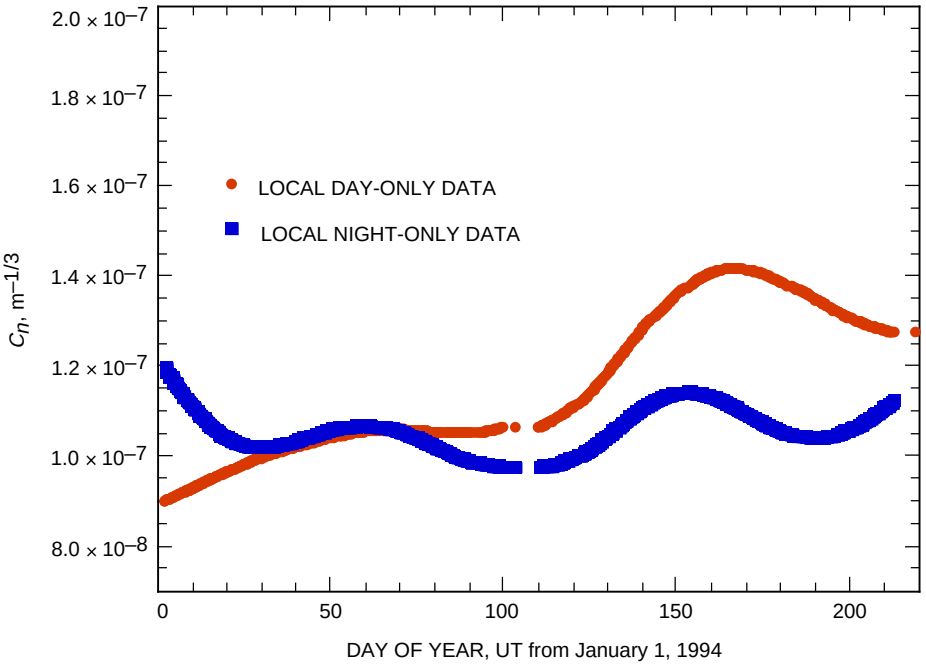

Fig. 8. Goldstone night and day C_n variations, smoothed C_n values.

C_n estimates, I have taken the 200-second ASD measurements of Fig. 6(a) in [8] to derive C_n values. The WVR data are divided into a night (12 p.m. through 8 a.m. local time) and a 24-hour time series. Figure 9 shows a comparison of both the day and night GPS time series and the WVR time series. Surprisingly, both data sets show that the difference between the day and night C_n variation becomes negligible in the winter months. A significant difference in the two data sets becomes apparent during the summer months. Although both data sets show that the daytime fluctuations become larger than the nighttime fluctuations during the summer months, the WVR data suggest that the day–night difference is approximately 50 percent, whereas the GPS data suggest a day–night difference of approximately 25 percent. Although additional comparisons need to be made, this difference may suggest that an improvement in the C_n extraction procedure could be made. It may be that the GPS global filtering and estimation routines used in the GPS Flinn data reduction are absorbing some fraction of the seasonal tropospheric fluctuations into other parameters. Because nontropospheric contributions to the residuals have a different spatial and temporal dependence, it might be possible to solve for the component of the residuals that has the correct functional form, thus improving the extraction process.

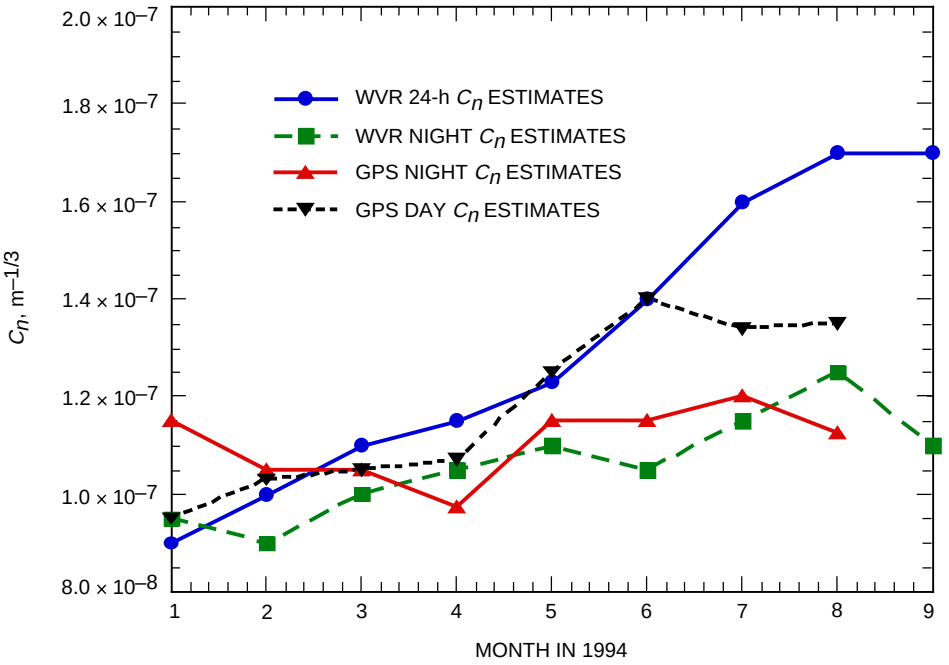

Fig. 9. A comparison of WVR and GPS C_n.

VI. Mean Wet Refractivity Model

The relationship between the structure constant, C_n, and the variance of the index of refraction fluctuation [7] is

$$C_n \propto \sqrt{\langle n_1^2 \rangle} \tag{12}$$

where n_1 is the index of refraction fluctuation and is related to n, the index of refraction, as

$$n = \langle n \rangle (1 + n_1)$$

Refractivity is related to the index of refraction by

$$\chi = (n-1) \times 10^6 \tag{13}$$

Recent tropospheric scintillation experiments have shown strong correlation between $\langle n_1^2 \rangle$ and $\langle \chi_{wet} \rangle$ (i.e., $\langle n_1^2 \rangle \propto \langle \chi_{wet} \rangle$ [11]). Refractivity is given by

$$\chi = \chi_{dry} + \chi_{wet} \cong 77.6 \frac{P_D}{T} - 12.8 \frac{P_V}{T} + 3.776 \times 10^6 \frac{P_V}{T^2} \tag{14}$$

where P_D is the partial pressure of dry air in mbar, P_V is the water vapor pressure in mbar, and T is temperature in Kelvin. Using surface meteorological data, an estimate of the mean wet and dry refractivity can easily be obtained. The weakness, however, is that the surface meteorological data do not always correspond to the true troposphere weather conditions at high altitude. Various studies of surface meteorological data and phase fluctuations in radio interferometry found that there is strong correlation with temperature and direct sunlight duration but anticorrelation with cloud cover [12]. Thus, under ideal conditions, we may expect a good correlation of C_n and refractivity calculated with the surface meteorological parameters.

An estimate of C_n based on a mean refractivity model using surface meteorological data has been made for the Goldstone site during the 10-day period in June 1994. As in [11], a linear relationship between wet refractivity and C_n is assumed. In addition, since dry refractivity can sometimes contribute as much as approximately 20 percent of the tropospheric delay fluctuations, a dry refractivity term, $\chi_{dry} - \langle \chi_{dry} \rangle$, is also included in the model, along with a lag term. The modified model is as follows:

$$C_n(t) = A[\chi(t - lag) - B] \tag{15}$$

where the constants A, B, and lag were obtained by linear regression techniques. The lag term accounts for the thermal inertia of the atmosphere, and B is a bias that is approximately equal to $\langle \chi_{dry} \rangle$. For the June 1994 period, the model parameters were found to be $A = 1.8 \times 10^{-9}$, $B = 206.9$, and $lag = 8.0$ hours. This model is shown as the solid curve in Fig. 6(a), along with the GPS-derived C_n values for the same period. A very reasonable agreement is observed between the two data sets. Both show a strong diurnal dependence and the point-to-point fluctuations in both data sets are well correlated.

VII. Summary

This article discussed a method of extracting tropospheric fluctuation statistics from the GPS Flinn database. The elevation and site dependence of the GPS residuals were approximately what is expected from tropospheric fluctuations. The GPS residuals were found to have temporal and probability density statistics similar to those expected from Kolmogorov turbulence models of the troposphere.

The tropospheric turbulence parameter, C_n, was extracted from the GPS Flinn database. The absolute magnitudes of C_n were in general agreement with both WVR and VLBI measurements. The long-term average C_n value differed from site to site, with the drier sites (Goldstone and Alberthead) having C_n values approximately 50 percent of the value at wet sites (Fortaleza and Kourou). Strong diurnal C_n variations of 25 to 50 percent were found in agreement with recent WVR measurements. The diurnal variations were found to be seasonally dependent, with almost no difference being observed during the winter months. A mean wet refractivity model, known to correlate strongly with the seasonal tropospheric fluctuations, was shown to be consistent with the GPS C_n measurements for a 10-day time period during the summer of 1994 in Goldstone.

Direct comparisons with WVR estimates of the tropospheric fluctuations suggest that the GPS extraction technique is not yet optimized. The GPS C_n estimate seems to be underestimating the maximum summer seasonal fluctuation by perhaps as much as 50 percent. An elevation and frequency filter was suggested as the next step in optimizing the C_n extraction algorithm.

This technique of estimating the tropospheric turbulence parameter, C_n, using the GPS Flinn residuals seems very promising. However, before a statistical model of the systematic C_n variations is developed, the C_n extraction algorithm should be improved and a long-term (a year or more) comparison with WVR data (at the same site) be undertaken.

Acknowledgments

The author would like to thank the following for their assistance: Roger Linfield for his original ideas, advice, and thorough reading of this article; Gabor Lanyi for his criticism and discussion of the results; Chris Jacobs for his many analysis ideas; and David Jefferson for assistance in the use and understanding of the GPS Flinn data files.

References

[1] R. N. Treuhaft and G. E. Lanyi, "The Effect of the Dynamic Wet Troposphere on Radio Interferometric Measurements," *Radio Science*, vol. 22, pp. 251–265, 1987.

[2] A. Praskovsky and S. Oncley, "Probability Distribution Of Velocity Differences at Very High Reynolds Numbers," *Physical Review Letters*, vol. 73, pp. 3399–3402, 1995.

[3] D. Schertzer and S. Lovejoy, *Non-Linear Variability in Geophysics*, Boston, Massachusetts: Kluwer Academic Publishers, pp. 269–280, 1991.

[4] C. C. Chao, *The Troposphere Calibration Model For Mariner Mars 1971*, JPL Technical Report 32-1587, Jet Propulsion Laboratory, Pasadena, California, pp. 61–76, March 1974.

[5] A. Juneja, D. P. Lathrop, K. R. Sreenivasan, and G. Stolovitzky, "Synthetic Turbulence," *Phy. Rev. E.*, vol. 49, pp. 5179–5194, 1994.

[6] V. I. Tatarski, *Wave Propagation in a Turbulent Medium*, New York: Dover, 1961.

[7] A. Ishimaru, *Wave Propagation and Scattering in Random Media*, New York: Academic Press, pp. 528–543, 1978.

[8] S. J. Keihm, "Water Vapor Radiometer Measurements of the Tropospheric Delay Fluctuations at Goldstone Over a Full Year," *The Telecommunications and Data Acquisition Progress Report 42-122, April–June 1995*, Jet Propulsion Laboratory, pp. 1–11, Pasadena, California, August 15, 1995.
http://tda.jpl.nasa.gov/tda/progress_report/42-122/122J.pdf

[9] W. H. Press, B. P. Flanney, S. A. Taukolsky, and W. T. Vetterling, *Numerical Recipes*, New York: Cambridge University Press, pp. 430–435, 1989.

[10] R. A. Sramek, "Atmospheric Phase Stability at the VLA," presented at the URSI-IAM Symposium on Radio Astronomical Seeing, Beijing, China, May 15–19, 1989.

[11] Y. Karasawa, K. Yasukawa, and M. Yamada, "Tropospheric Scintillation in the 14–11 GHz Bands on Earth–Space Paths With Low Elevation Angles," *IEEE Transactions on Antennas and Propagation*, vol. 36, pp. 563–569, 1988.

[12] R. A. Hinder, "Fluctuations of Water Vapor Content in the Troposphere as Derived From Interferometric Observations of Celestial Radio Sources," *J. Atmos. Terr. Phys.*, vol. 34, pp. 1171–1186, 1972.

[13] F. Schmitt, D. Lavallee, and D. Schertzer, "Empirical Determination of Universal Multifractal Exponents in Turbulent Velocity Fields," *Physical Review Letters*, vol. 68, pp. 305–308, 1995.

[14] E. E. Peters, *Fractal Market Analysis*, New York: John Wiley and Sons Inc., pp. 210–214, 1994.

Appendix A

Levy–Pareto Distribution Function and Turbulence

The Levy–Pareto distributions are stable distributions and are sometimes called stable Levy distributions or stable Paretain distributions. A probability density function, $f(x)$, can be obtained by a Fourier transform of its characteristic function, $L(t)$. A probability density function is stable if there exists a $b > 0$ for all $b_1 > 0$ and $b_2 > 0$ such that

$$L(b_1 t) \times L(b_2 t) = L(bt) \tag{A-1}$$

This means that the distributions all have the same "shape." Two well-known stable distributions are the Gaussian and Cauchy distributions. Both are special cases of the Levy distribution. The Levy characteristic function is defined as

$$\left.\begin{aligned} L(t) &= \exp\left\{ i\delta t - |\gamma|^{\alpha} \left(\frac{1 - i\beta t}{|t|} \right) \tan\frac{\pi\alpha}{2} \right\} \qquad \alpha \neq 1 \\ &= \exp\left\{ i\delta t - |\gamma|^{\alpha} \left(1 - i\beta \frac{2}{\pi} \ln(|t|) \right) \right\} \qquad \alpha = 1 \end{aligned}\right\} \tag{A-2}$$

The distribution has four parameters, α, β, γ, and δ. Where δ is the location parameter, typically $\delta = 0$, when the mean exists ($\alpha > 0$) $\delta =$ mean. The scale parameter is γ and is a measure of dispersion; it is related to the standard deviation of the normal distribution by a factor of $1/\sqrt{2}, \gamma > 0$. The skewness parameter is β, is between $+1$ and -1, and typically is zero. For a symmetrical distribution, $\beta = 0$.

The primary parameter is the characteristic exponent α, which determines the flatness of the tails of the distribution; thus, the finiteness of the moments of the distribution critically depends upon this exponent. When $\alpha = 2, \beta = 0, \gamma = \sigma/\sqrt{2}$, and $\delta = 0$, the distribution is Gaussian. For a Cauchy distribution, $\alpha = 1, \beta = 0, \gamma =$ interquartile range, and $\delta =$ median. Now an important property of the Levy distribution is that, for $\beta = 0$, the tail of the survival function, $S(x)$ [$1 - F(x)$, where $F(x)$ is the cumulative distribution function], follows the law of Pareto:

$$S(x > c) = \left(\frac{c}{x}\right)^{-\alpha} \qquad c > \sigma \tag{A-3}$$

This simply states that the probability of finding a value of x greater than a constant c goes as a power law with the exponent $-\alpha$.

The Levy distribution is connected to turbulence through the law of Pareto. A considerable body of empirical and theoretical evidence supports the scale invariant and intermittency cascade model of turbulence [3,13]. This model is limited by an inner scale ($\sim$cm) and an outer scale (>1000 km) and is characterized by two critical exponents, H and α. The scaling exponent, H, usually named the Hurst exponent, relates the fluctuations $\Delta X(\Delta t)$ in field $X(t), \Delta X(\Delta t) = X(t + \Delta t) - x(t)$, at large and small scales, explicitly:

$$P\left\{\Delta X\left(\frac{\Delta t}{p}\right)\right\} = P\left\{\frac{\Delta X(\Delta t)}{p^H}\right\} \tag{A-4}$$

where $P\{z(t)\}$ is the probability density function of the field $z(t)$ and $p > 1$. This simply means that decreasing the scales by a factor of p decreases the fluctuations by p^H. The relationship between the Hurst exponent, H, and the power law slope, B, of the time-series power density spectra is $B = 1 + 2H$ [5]. Thus, the Hurst exponent can be trivially obtained from the power density spectra.

The second critical exponent, α, characterizes the extreme fluctuations (the intermittency), and the survival function follows a hyperbolic functional form first proposed by Mandelbrot:

$$S(\Delta X > c) \propto \left(\frac{c}{\Delta X}\right)^{-\alpha} \qquad c \to \infty \tag{A-5}$$

The relationship between the two critical exponents of classical turbulence and the scaling behavior for the statistical moments can be obtained:

$$\langle \Delta X(\Delta t)^q \rangle = \int [\Delta X]^q P(\Delta X) d[\Delta X] \propto \Delta t^{k(q)} \tag{A-6}$$

where the angle brackets represent ensemble averaging, q is the moment order, and $k(q)$ is a scaling exponent dependent upon the moment order and the probability density function of the turbulence (α and H scaling). For the classical Kolmogorov turbulence theory (sometimes referred to as K41), a simple relationship exists (for the second-order moment, $q = 2$) between the probability space exponent, α; the temporal scaling exponent, H; and the statistical structure function exponent [13,14]: $k(q = 2) = 2H = 2/\alpha$. For Kolmogorov turbulence, both the temporal structure function exponent ($q = 2$ for $\Delta t > 200$ seconds) and the ASD have power law exponents of 2/3 [1]. Thus, we expect H=1/3, B=5/3, and $\alpha = 3.0$ for Kolmogorov turbulence.

Appendix B
GPS Zenith Tropospheric Delay Variance

The variance of a random function of time, $f(t)$, over an interval, T, is

$$\sigma^2(T) = \frac{1}{T^2}\int (T-t)D_f(t)dt \tag{B-1}$$

where $D_f(t)$ is the structure function of f and the limits of integration are from 0 to T. If we define the satellite-averaged zenith delay as

$$P = f(t) = \frac{1}{N}\sum \tau_i(t)m_i[\theta(t)], \quad i = 1, 2, 3, \cdots, N \tag{B-2}$$

where i is one of the N visible satellites, $m(\theta)$ is the mapping function ($\sim\sin\theta$, see [4]), $\tau(t)$ is the tropospheric delay along the direction of the satellite, and $\tau(t)$ is given as

$$\tau = \frac{1}{m(\theta)}\int \chi[\mathbf{x} + \mathbf{r}(\theta, \varphi, z)]dz \tag{B-3}$$

where χ is the refractivity, $\mathbf{x}$ is the coordinate vector of the site in question, and $\mathbf{r}$ is the vector along the direction of the satellite at elevation θ and azimuth φ with a projection along the vertical axis of z, then the structure function of the satellite-averaged zenith tropospheric delay is given as

$$D_p(\Delta t) = \langle [P(t+\Delta t) - P(t)]^2 \rangle \tag{B-4}$$

where the angle brackets denote an ensemble averaging. Combining Eqs. (B-2) through (B-4) and interchanging the ensemble averaging and the integrations obtains

$$D_p(\Delta t) = \sum_{ij}\frac{1}{N^2}\iint \left[\langle \chi(\mathbf{r}_i, t+\Delta t)\chi(\mathbf{r}_j, t+\Delta t)\rangle + \langle \chi(\mathbf{r}_i, t)\chi(\mathbf{r}_j, t)\rangle - 2\langle \chi(\mathbf{r}_i, t)\chi(\mathbf{r}_j, t+\Delta t)\rangle\right] dz_i dz_j \tag{B-5}$$

where both i and j range from 1 to N. The z integration ranges from 0 to h, where h is the effective height of the troposphere.

The frozen flow assumption states that the temporal fluctuations are caused by spatial fluctuations that are moved past the site by the wind. If the medium is stationary in time and homogeneous in space, then for a random function, f,

$$f(\mathbf{r}, t) = f(\mathbf{r} + \mathbf{v}t) \tag{B-6}$$

where $\mathbf{v}$ is the wind velocity. The correlation function for f may then be written as

$$\langle f(\xi,t_i)f(\zeta,t_j)\rangle = \langle f(\xi+\mathbf{v}t_i)f(\zeta+\mathbf{v}t_j)\rangle = \langle f(\xi-\zeta+\mathbf{v}(t_i-t_j))f(0)\rangle \tag{B-7}$$

This allows Eq. (B-5) to be reduced to

$$D_p(\mathbf{v}\Delta t) = \sum_{ij}\frac{1}{N^2}\iint\left[2\langle\chi(\eta)\chi(0)\rangle - 2\langle\chi(\eta+\mathbf{v}\Delta t)\chi(0)\rangle\right]dz_i dz_j \tag{B-8}$$

where $\eta = \mathbf{r}_i - \mathbf{r}_j$. In addition, the approximation that $\mathbf{r}_j(t) = \mathbf{r}_j(t+\Delta t)$ has been made for computational simplicity. This approximation is negligible for small Δt, those GPS interval times for which the distance moved by a satellite is small compared with the distances between the satellites.

Using Eq. (A-3) from [1], which is

$$\langle\chi(\mathbf{x}_1)\chi(\mathbf{x}_2)\rangle = \langle\chi^2\rangle - \frac{1}{2}D_\chi(|\mathbf{x}_1-\mathbf{x}_2|) \tag{B-9}$$

Eq. (B-8) is reduced to

$$D_p(|\mathbf{v}|\Delta t) = \sum_{ij}\frac{1}{N^2}\iint\left[D_\chi(|\eta+\mathbf{v}\Delta t|) - D_\chi(|\eta|)\right]dz_i dz_j \tag{B-10}$$

where both i and j range from 1 to N. Using Eqs. (B-10) and (B-1), an estimate for the zenith tropospheric delay variance can be written as

$$\sigma^2(zenith) = \frac{1}{T^2}\int(T-t)\sum_{ij}\frac{1}{N^2}\iint\left[D_\chi(|\eta+\mathbf{v}\Delta t|) - D_\chi(|\eta|)\right]dz_i dz_j dt \tag{B-11}$$

Thus, this estimate of the zenith tropospheric delay fluctuation is a temporal estimate over the interval T and a spatial estimate over all the visible satellites during interval T. The primary assumption of the Kolmogorov turbulence theory in the frozen flow model is that the structure function depends only upon a displacement vector:

$$D_\chi(|\mathbf{R}|) = \langle[\chi(\mathbf{r}+\mathbf{R}) - \chi(\mathbf{R})]^2\rangle = \frac{\left(C_n R^{1/3}\right)^2}{1+(R/L)^{2/3}} \tag{B-12}$$

where C_n is the structure constant, which characterizes the rockiness of the spatial inhomogeneity; L is the saturation length, typically ~3000 km; and $R = |\mathbf{R}|$. The coordinate vectors η and $\mathbf{v}$ (lateral wind) may be expressed in terms of θ, φ, and z as

$$\begin{aligned}|\eta| &= |\mathbf{r}_i - \mathbf{r}'_j| \\ &= [z_i\cot(\theta_i)\cos(\varphi_i) - z'_j\cot(\theta_j)\cos(\varphi_j)]^2 + [z_i\cot(\theta_i)\sin(\varphi_i) - z'_j\cot(\theta_j)\sin(\varphi_j)]^2 + [z_i - z'_j]^2\end{aligned} \tag{B-13}$$

and

$$|\eta + \mathbf{v}\Delta t| = |\mathbf{r}_i - \mathbf{r}'_j + \mathbf{v}\Delta\mathbf{t}| = \ [z_i \cot(\theta_i)\cos(\varphi_i) - z'_j \cot(\theta_j)\cos(\varphi_j) + |v_x \Delta t|]^2$$

$$+ [z_i \cot(\theta_i)\sin(\varphi_i) - z'_j \cot(\theta_j)\sin(\varphi_j) + |v_y \Delta t|]^2 + [z_i - z'_j]^2 \qquad \text{(B-14)}$$

Using the GPS Flinn database and Eqs. (B-11) through (B-14), a direct calculation of σ_{theory} at a given time, t, can be made. To calculate $\sigma_{residuals}$, the rms of P [Eq. (B-2)] is calculated over a sampling time, T, where we replace $\tau_i(t)_{res}$ for $\tau_i(t)$. Then, using Eq. (11), C_n can be extracted. Since even for short sampling times some tropospheric fluctuations are absorbed in the GPS estimated parameter, $\tau_z(t)$, the zenith troposphere delay, additional accuracy could be obtained by using Eq. (4) over a suitable interval; this has been left for future study.